Available online at www.sciencedirect.com
SCIENCE DIRECT®
International Journal of Thermal Sciences 43 (2004) 201–211
International Journal of Thermal Sciences
www.elsevier.com/locate/ijts

Application of low Reynolds number k–ε turbulence models to the study of turbulent wall jets

Jamel Kechiche [a], Hatem Mhiri [a], Georges Le Palec [b,*], Philippe Bournot [b]

[a] *Laboratoire de mécanique des fluides et thermique, École nationale d'ingénieurs de Monastir, route de Ouardanine, 5000 Monastir, Tunisia*
[b] *Institut de mécanique de Marseille, 60, rue Joliot-Curie, technopôle de Château-Gombert, 13453 Marseille cedex 13, France*

Received 25 September 2002; accepted 17 June 2003

Abstract

In this work, we use closure models called "low Reynolds number k–ε models", which are self-adapting ones using different damping functions, in order to explore the computed behavior of a turbulent plane two-dimensional wall jets. In this study, the jet may be either isothermal or submitted to various wall boundary conditions (uniform temperature or a uniform heat flux) in forced convection regime. A finite difference method, using a staggered grid, is employed to solve the coupled governing equations with the inlet and the boundary conditions. The predictions of the various low Reynolds number k–ε models with standard or modified C_μ adopted in this work were presented and compared with measurements and numerical results found in the literature.

Keywords: Wall jet; Turbulent; Low Reynolds number; k–ε model; Modified C_μ; Shear stress; Uniform heat flux; Forced convection; Stanton number

1. Introduction

A turbulent wall jet is obtained by injecting a fluid at a high velocity tangentially to a flat plate boundary. The resulting flow can be viewed as a combination of an inner wall boundary layer, where the velocity increases from zero at the wall to a local maximum, and an outer free jet where the flow decreases from a local maximum to zero (or the free stream value in the case of moving surroundings). The strong interaction between these two layers causes the complexity of this type of flow.

Wall jets occur in many industrial applications such as solid smoothing, inlet devices in ventilation and optimization of the film cooling of gas turbine blades. For this reason, the turbulent wall jet has been the subject of several experimental studies for both the isothermal case [1–7] and the non-isothermal case [8–10].

In a numerical study, solutions of this type of flow were obtained for the laminar regime by using a change of variables which caused the flow conditions at the nozzle exit to be ignored [11]. However, using direct resolution of the two-dimensional Navier Stokes equations, the authors of [12] took into account these conditions. The numerical solution of the governing equations is more complicated in turbulent regime because additional terms appear in the equations and lead to a loss of information which makes it necessary to compensate by using physical assumptions called closure assumptions. The set of model equations recommended by Launder and Spalding [13] has been most widely employed. This model was established for high Reynolds numbers flows where viscous effects are negligible compared to the turbulent ones. For wall jets, the viscous layer plays an important role in heat and momentum transfer. In this region, molecular viscosity is not negligible and the use of this model allows the resolution of the equations starting only from one well-defined distance of the wall at a point located out of the viscous layer. Thereafter, new formulations are necessary to complete the solution and to determine the conditions at the points where calculation begins [1,9].

Ljuboja and Rodi [14] had shown that for a two-dimensional turbulent wall jet, this model associated to wall laws produces a spreading rate more than 30% higher than the experimental results [1]. Indeed, this modeling does not take into account the damping effect of the wall on the

* Corresponding author.
E-mail addresses: Jamel.Kechiche@enim.rnu.tn (J. Kechiche), hatem.mhiri@enim.rnu.tn (H. Mhiri), Lepalec@unimeca.univ-mrs.fr (G. Le Palec), Bournot@unimeca.univ-mrs.fr (Ph. Bournot).

1290-0729/$ – see front matter
doi:10.1016/j.ijthermalsci.2003.06.005

Nomenclature

b	slot width of the jet nozzle	m
C_f	friction coefficient ($2\tau_w/\rho u_m^2$)	
c_p	specific heat at constant pressure	$J{\cdot}kg^{-1}{\cdot}K^{-1}$
$C_\mu, C_{\varepsilon 1}, C_{\varepsilon 2}$	turbulent model constants	
D, F	additional terms in Eqs. (4) and (5)	
f_μ, f_1, f_2	model functions of low Reynolds turbulence k–ε model	
J	kinematic momentum flux ($u_0^2 b$)	$m^3{\cdot}s^{-2}$
h	local heat transfer coefficient	$W{\cdot}m^{-2}{\cdot}K^{-1}$
k	turbulent kinetic energy	$m^2{\cdot}s^{-2}$
Nu_{x_1}	local Nusselt number (hx_1/λ)	
Pr	Prandtl number ($\mu c_p/\lambda$)	
Pr_t	turbulent Prandtl number	
Re	Reynolds number ($u_0 b/\nu$)	
Re_t	turbulence Reynolds number ($k^2/\nu\tilde{\varepsilon}$)	
Re_k	dimensionless distance ($y\sqrt{k}/\nu$)	
Re_τ	dimensionless distance (yu_τ/ν)	
Re_{x_1}	local Reynolds number ($u_m x_1/\nu$)	
St	local Stanton number ($h/\rho c_p u_m$)	
T	mean temperature	K
T_f	friction temperature ($\Phi/\rho c_p u_\tau$)	K
T^+	dimensionless temperature ($T_w - T/T_f$)	
u, v	mean velocity components along x and y directions	$m{\cdot}s^{-1}$
U, V	Dimensionless velocity components	
u_τ	friction velocity ($\sqrt{\tau_w/\rho}$)	$m{\cdot}s^{-1}$
u^+	dimensionless velocity (u/u_τ)	
x, y	longitudinal and transverse coordinates	m
X, Y	dimensionless longitudinal and transverse coordinates	
x_1	$x + 20b$	m
y^+	dimensionless length from wall ($u_\tau y/\nu$)	
$y_{1/2}$	jet half width	m

Greek symbols

α	thermal diffusivity of fluid (ν/Pr)	
$\varepsilon, \tilde{\varepsilon}$	dissipation rate of the turbulent kinetic energy, ($\tilde{\varepsilon} = \varepsilon - D$)	$m^2{\cdot}s^{-3}$
λ	thermal conductivity	$W{\cdot}m^{-1}{\cdot}K^{-1}$
ν	kinematic viscosity of fluid (μ/ρ)	$m^2{\cdot}s^{-1}$
ν_t	kinematic eddy viscosity	$m^2{\cdot}s^{-1}$
$\sigma_k, \sigma_\varepsilon$	empirical constants appearing in Eqs. (4) and (5)	
Φ	wall heat flux	$W{\cdot}m^{-2}$
τ_w	wall shear stress ($\mu[\partial u/\partial y]_{y=0}$)	

Subscripts

0	nozzle exit
a	dimensionless quantities
m	maximum velocity value
w	wall value
∞	fluid ambient

Superscript

$'$	fluctuation

lateral velocity fluctuations. To solve this problem, Ljuboja and Rodi [14] have proposed a modified version of the k–ε model [13]. The empirical constant in the Kolmogorov–Prandtl relation ($C_\mu = 0.09$) was replaced by a function which is derived by reducing a model from of the Reynolds stress transport equations to algebraic expressions, retaining the wall damping correction to the pressure strain model used in these equations. This procedure proved to predict wall jets with a sufficient accuracy for practical purposes.

The second order turbulence model, using transport equations for the Reynolds stresses [15], predict the wall jet correctly, when the wall influence on the pressure strain correlation appearing in the Reynolds stress equations is taken into account. Predictions with a Reynolds stress equation model not accounting for this influence, yielded a rate of spread which was still 20% too high [16].

For the three-dimensional turbulent wall jet, Launder [17] has noticed that the most striking feature of this flow is that the jet's lateral rate of spread (i.e., in the direction parallel to the wall) is much larger than the rate normal to the wall. This highly unequal rate of growth in the two directions arises from the creation of streamwise vorticity, rather than from anisotropic diffusion. Launder [17] showed that the numerical solutions, proposed by Kebede [18], using a linear eddy-viscosity model with wall functions, under-predicted the strength of the streamwise vorticity created and, consequently, did not accurately mimic the anisotropic spreading rates in the lateral and normal directions. Therefore computation of three-dimensional turbulent wall jet should be made with a second order turbulence models. The most recent study is presented by Craft and Launder [19]: these authors, proposed different numerical solutions for different models of the pressure strain correlation, in order to explain the cause of the high lateral rates of spread observed in experiments [20] compared to the rate normal to the wall.

This review of the aforementioned numerical studies shows that the turbulent wall jets were studied either with second order models, at high or at low Reynolds numbers [21], or with a first order models at high Reynolds numbers. Drawbacks of second order models remain in the correct interpretation of all the terms appearing in the equations and on the accurate definition of the boundary conditions, thus on the requirement of more memory and computing time. For the high Reynolds number turbulence models, molecular transport terms have been neglected yielding equations that are not valid in the viscous sublayer zone adjacent to the wall. Wall laws derived from experiments in the similarity region are thus used to complete the solution of the problem,

which implies that such a numerical resolution is possible only if experimental results are available for the studied configuration.

Closure self-adapting models, called "low Reynolds number k–ε turbulence models", using damping functions were developed by several researchers [22–24]. These models which are not associated with wall laws, made it possible to predict effectively the dynamic, thermal, and turbulent behavior of turbulent pipe and channel flows, flat plate boundary layer, and a diffuser flow, but were not tested for the turbulent wall jets. In the present study we propose to apply several of these turbulent models to the study of a plane two-dimensional wall jet in a quiescent surrounding which may be either isothermal or submitted to various wall boundary conditions (uniform temperature or uniform heat flux). The objective of this study is to describe both the momentum and heat transfer processes for this type of flow, in order to know if these types of models may be used to describe effectively the experimental results.

2. Equations and numerical method

2.1. Assumptions

Fig. 1(a) shows an incompressible jet discharged from a rectangular nozzle tangentially to a flat horizontal plate into uniform stagnant environment in forced convection. We assume that the width of the nozzle is very large compared to its thickness (b) and therefore we can consider the flow as a two-dimensional wall jet. We assume the jet at ambient temperature and the flat plate submitted to different boundary conditions (uniform heat flux or uniform temperature). The flow is turbulent, fully developed and stationary on average.

2.2. Mean flow equations

Under the assumption of a steady boundary layer flow (i.e., $u \gg v$, $\partial/\partial y \gg \partial/\partial x$), the governing equations for the velocity and temperature, in forced convection, are:

Conservation of mass

$$\frac{\partial u}{\partial x} + \frac{\partial v}{\partial y} = 0 \tag{1}$$

Conservation of momentum

$$u\frac{\partial u}{\partial x} + v\frac{\partial u}{\partial y} = \frac{\partial}{\partial y}\left(\nu\frac{\partial u}{\partial y} - \overline{u'v'}\right) \tag{2}$$

Conservation of energy

$$u\frac{\partial T}{\partial x} + v\frac{\partial T}{\partial y} = \frac{\partial}{\partial y}\left(\alpha\frac{\partial T}{\partial y} - \overline{v'T'}\right) \tag{3}$$

This system of Eqs. (1)–(3) contains more unknowns than equations, so it is an open system. Taking the average of an instantaneous equation leads to a loss of information which is replaced by closure assumptions.

2.3. Turbulence models

In the present work, the closure of averaged Eqs. (1)–(3) is ensured by different low Reynolds number k–$\tilde{\varepsilon}$ turbulence models [22–24]. The mean turbulent kinetic energy and its dissipation rate are given by the system of equations written in the following form:

$$u\frac{\partial k}{\partial x} + v\frac{\partial k}{\partial y} = \frac{\partial}{\partial y}\left(\left(\nu + \frac{\nu_t}{\sigma_k}\right)\frac{\partial k}{\partial y}\right) + \nu_t\left(\frac{\partial u}{\partial y}\right)^2 - \tilde{\varepsilon} - D \tag{4}$$

$$u\frac{\partial \tilde{\varepsilon}}{\partial x} + v\frac{\partial \tilde{\varepsilon}}{\partial y} = \frac{\partial}{\partial y}\left(\left(\nu + \frac{\nu_t}{\sigma_\varepsilon}\right)\frac{\partial \tilde{\varepsilon}}{\partial y}\right) + C_{\varepsilon 1} f_1 \frac{\tilde{\varepsilon}}{k}\nu_t\left(\frac{\partial u}{\partial y}\right)^2 - C_{\varepsilon 2} f_2 \frac{\tilde{\varepsilon}^2}{k} + F \tag{5}$$

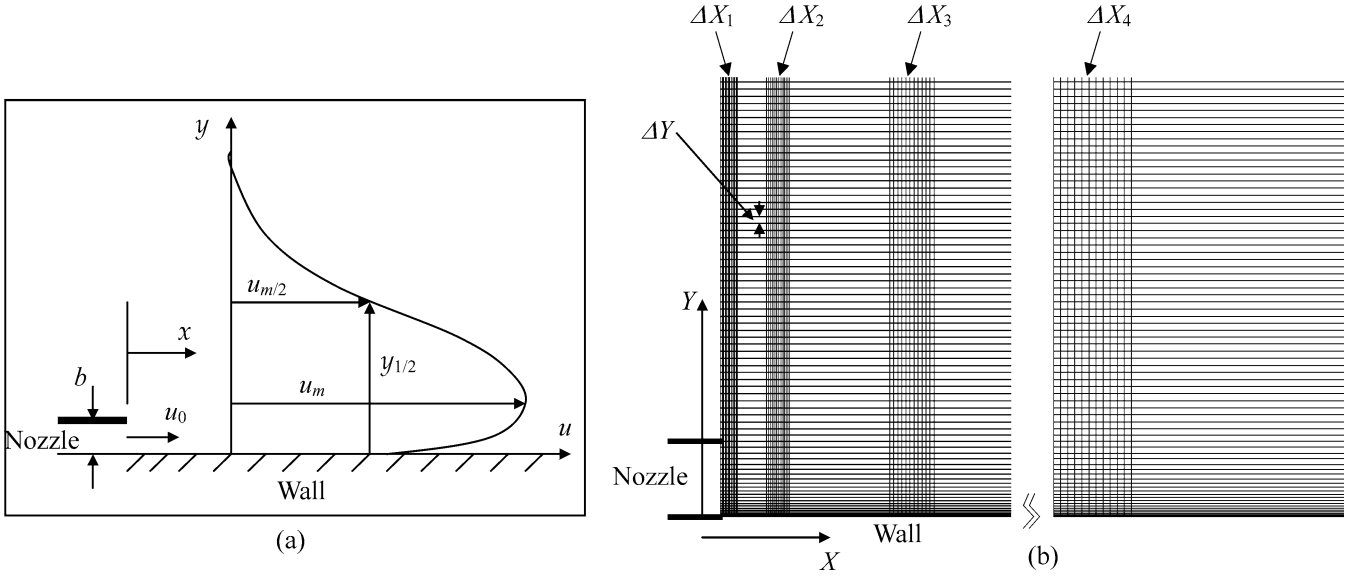

Fig. 1. Flow configuration (a) and representation of the grid (b).

The Reynolds stress $\overline{u'v'}$ and the heat flux $\overline{v'T'}$ appearing in the system of Eqs. (2)–(3) may be expressed as:

$$\overline{u'v'} = -\nu_t \frac{\partial u}{\partial y}, \qquad \overline{v'T'} = -\frac{\nu_t}{Pr_t}\frac{\partial T}{\partial y} \tag{6}$$

The eddy viscosity ν_t is related to k and $\tilde{\varepsilon}$ through the Kolmogorov–Prandtl relations as:

$$\nu_t = C_\mu f_\mu \frac{k^2}{\tilde{\varepsilon}} \tag{7}$$

σ_k, σ_ε, $C_{\varepsilon 1}$ and $C_{\varepsilon 2}$ are empirical constants and f_1, f_2 and f_μ are the turbulence model functions for the near wall formulation. Table 1 summarizes these constants and functions including additional terms D and F appearing in the system of Eqs. (4)–(5) for three low Reynolds number turbulence models used in this work.

It is noted that the evaluation of the dissipation rate of the turbulent kinetic energy on the wall is the major problem of the modeling of flows attached to obstacles. Two approaches were adopted to solve this problem. The first one [22] consists in imposing a null wall gradient for ε and $D = 0$, whereas the second one uses an additional term D [23,24] (Table 1) in the transport k Eq. (4), which is chosen to impose the boundary condition $\tilde{\varepsilon} = 0$ ($\tilde{\varepsilon} = \varepsilon - D$) at the wall.

For the modeling of the generation term of ε in the vicinity of the wall, Herrero et al. [22] used an empirical damping function f_1, whereas Nagano and Hishida [23] and Chien [24] proposed the use of an additional empirical term F in the transport equation of ε. f_2 is a function which corrects the destruction term of ε in low Reynolds turbulence flow. This term goes quickly to a high turbulence form because f_2 rapidly approaches 1 with the increase of local turbulence Reynolds numbers.

2.4. Boundary conditions

The statement of the problem is achieved with the formulation of inlet conditions at the nozzle and boundary conditions:

$$\text{For } x = 0 \quad \begin{cases} 0 < y < b: \quad u = u_0;\ v = 0;\ k = k_0; \\ \quad \tilde{\varepsilon} = \tilde{\varepsilon}_0;\ T = T_\infty \\ y \geqslant b: \quad u = 0;\ v = 0;\ k = 0; \\ \quad \tilde{\varepsilon} = 0;\ T = T_\infty \end{cases}$$

$$\text{For } x > 0 \quad \begin{cases} y = 0: \quad u = 0;\ v = 0;\ k = 0 \\ \text{Wall submitted to a uniform heat flux:} \\ \quad \frac{\partial (T - T_\infty)}{\partial y} = -\frac{\Phi}{\lambda} \\ \text{Wall submitted to a uniform temperature:} \\ \quad T = T_w \\ y \to \infty: \quad u = 0;\ k = 0;\ \tilde{\varepsilon} = 0;\ T = T_\infty \end{cases} \tag{8}$$

Table 1
Constants and functions used in low Reynolds number turbulence models

Models	$\tilde{\varepsilon}_w$	C_μ	$C_{\varepsilon 1}$	$C_{\varepsilon 2}$	σ_k	σ_ε	f_μ	f_1	f_2	D	F
Chien [24]	0	0.09	1.35	1.8	1.0	1.3	$1 - \exp(-0.0115y^+)$	1.0	$1 - 0.22\exp[-(Re_t/6)]^2$	$2\nu k/y^2$	$-2(\varepsilon\nu/y^2) \times \exp(-0.5y^+)$
Nagano and Hishida [23]	0	0.09	1.45	1.9	1.0	1.3	$[1 - \exp(-y^+/26.5)]^2$	1.0	$1 - 0.3\exp(-Re_t^2)$	$2\nu(\frac{\partial\sqrt{k}}{\partial y})^2$	$\nu\nu_t(1 - f_\mu)(\frac{\partial^2 u}{\partial y^2})^2$
Herrero et al. [22]	$\frac{\partial\varepsilon}{\partial y} = 0$	0.09	1.44	1.92	1.0	1.3	$[1 - \exp(-0.0066Re_k)]^2$ $\times[1 + 500\exp(-0.0055Re_k)/Re_t]$	$1 + (\frac{0.05}{f_\mu})^2$	$1 - (0.3/B)\exp(-Re_t^2)$ $B = 1 - 0.7\exp(-Re_k)$	0	0

2.5. Dimensionless equations

Let us introduce the following dimensionless variables:

$$X=\frac{x}{b},\quad Y=\frac{y}{b},\quad U=\frac{u}{u_0},\quad V=\frac{v}{u_0},$$
$$K=\frac{k}{u_0^2},\quad \widetilde{E}=\frac{\tilde{\varepsilon}b}{u_0^3} \tag{9}$$

- For a uniform heat flux boundary condition to the wall: $\theta=\frac{T-T_\infty}{\Phi b}\lambda$.
- For a uniform temperature boundary condition to the wall: $\theta=\frac{T-T_\infty}{T_w-T_\infty}$.

By using the above dimensionless variables, the system of Eqs. (1)–(5) can be transformed into the following forms:

$$\frac{\partial U}{\partial X}+\frac{\partial V}{\partial Y}=0 \tag{10}$$

$$U\frac{\partial U}{\partial X}+V\frac{\partial U}{\partial Y}=\frac{\partial}{\partial Y}\left[\left(\frac{1}{Re}+\nu_T\right)\frac{\partial U}{\partial Y}\right] \tag{11}$$

$$U\frac{\partial \theta}{\partial X}+V\frac{\partial \theta}{\partial Y}=\frac{\partial}{\partial Y}\left[\left(\frac{1}{Re\,Pr}+\frac{\nu_T}{Pr_t}\right)\frac{\partial \theta}{\partial Y}\right] \tag{12}$$

$$U\frac{\partial K}{\partial X}+V\frac{\partial K}{\partial Y}=\frac{\partial}{\partial Y}\left[\left(\frac{1}{Re}+\frac{\nu_T}{\sigma_k}\right)\frac{\partial K}{\partial Y}\right]+\nu_T\left(\frac{\partial U}{\partial Y}\right)^2-\widetilde{E}-D_a \tag{13}$$

$$U\frac{\partial \widetilde{E}}{\partial X}+V\frac{\partial \widetilde{E}}{\partial Y}=\frac{\partial}{\partial Y}\left(\left(\frac{1}{Re}+\frac{\nu_T}{\sigma_\varepsilon}\right)\frac{\partial \widetilde{E}}{\partial Y}\right)+C_{\varepsilon 1}f_1\frac{\widetilde{E}}{K}\nu_T\left(\frac{\partial U}{\partial Y}\right)^2-C_{\varepsilon 2}f_2\frac{\widetilde{E}^2}{K}+F_a \tag{14}$$

and:

$$\nu_T=C_\mu f_\mu\frac{K^2}{\widetilde{E}}$$

The dimensionless inlet and boundary conditions are written in the following way:

$$\text{For } X=0\quad\begin{cases}0<Y<1:\quad U=1;\ V=0;\ K=0.01;\\ \quad\widetilde{E}=0.0016;\ \theta=0\\ Y\geqslant 1:\quad U=0;\ V=0;\ K=0;\\ \quad\widetilde{E}=0;\ \theta=0\end{cases}$$
$$\text{For } X>0\quad\begin{cases}Y=0:\quad U=0;\ V=0;\ K=0\\ \text{Wall submitted to a uniform heat flux:}\\ \quad(\frac{\partial\theta}{\partial Y})_w=-1\\ \text{Wall submitted to a uniform temperature:}\\ \quad\theta_w=1\\ Y\to\infty:\quad U=0;\ K=0;\ \widetilde{E}=0;\ \theta=0\end{cases} \tag{15}$$

2.6. Numerical method of solution

The system of dimensionless equations (10)–(14) associated with the boundary and the inlet conditions (15) are solved by a finite difference method using a staggered grid. The momentum, energy, turbulent kinetic energy K and dissipation rate of turbulent kinetic energy $\widetilde{E}$ equations, are discretized at node $(i, j+1/2)$, while the continuity equation is discretized at node $(i+1/2, j+1/2)$. This method was adopted in previous works [12,25,26] in order to save numerical stability as compared with non-staggered grid method.

A non-uniform grid is used in the transverse direction of the flow (Fig. 1(b)). Spacing between two nodes (ΔY) is predicted by the following relation: $\Delta Y_j = a * \Delta Y_{j-1}$. The index j indicates the number of the node counted starting from the wall. The value of ΔY_1 which is the distance from the first node to the wall, is defined in order to have y^+ lower than 0.1 located in the viscous sublayer region where the flow is managed by the molecular viscosity of the fluid. Preliminary tests showed that when we choose the factor $a = 1.01$, we obtain at least 50 grid nodes for $y^+ < 11.5$ in the vicinity of the wall. This condition ensures that the viscous sublayer is well seized in the field of calculation. From the node number 465, the distance between two nodes becomes constant $(\Delta Y = 10^{-2})$ which allows to impose a sufficient number of grid points in this direction so that the jet is not cut $(Y_\infty = 37)$ until a distance $X = 160$.

In the longitudinal direction, the used grid is also non-uniform. Indeed, the step of calculation is taken very small in the vicinity of the nozzle $\Delta X_1 = 10^{-8}$, then, as the jet moves away from the source, the calculation step is increased gradually $(\Delta X_2 = 10^{-6},\ \Delta X_3 = 10^{-4})$. In order to be able to go farther in the jet, the last adopted step is $\Delta X_4 = 10^{-2}$.

The effect of this method of a first order accuracy is negligible on the results. In fact, preliminary computation was carried out with finer mesh than used in this work and the maximum difference between velocity results is of 3%.

The convergence of the solution is assumed to be reached when the relative change of velocity U between two successive iterations is lower than 10^{-7} for each node of the grid.

3. Results and discussions

3.1. Isothermal turbulent wall jet

3.1.1. Average characteristics of the flow

In this part, we present an analysis of the behavior of an isothermal wall jet in turbulent regime by discussing the validity of low Reynolds number turbulence models used in our numerical study. The calculations were started at the nozzle exit $(X = 0)$ with uniform velocity profile and uniform distribution of the kinetic energy and its dissipation rate. The results obtained far from the nozzle show that the mean and turbulence quantities attain similarity, and the half width grows linearly with the streamwise distance X so that $dY_{1/2}/dX$ is constant. In Table 2, the computed values of $dY_{1/2}/dX$ obtained by the different low Reynolds number turbulence models, are presented and compared with

those proposed numerically by Ljuboja and Rodi [14] and experimentally by Tailland [1].

It is noticed that the high Reynolds numbers turbulence model associated with wall law overestimates the expansion of the jet by approximately 30% [14]. By using low Reynolds number turbulence models, our numerical results approach those proposed experimentally by Tailland [1], but an overestimate of the jet expansion still occurs.

In order to correct the overestimation of the jet expansion, we modified the eddy viscosity correlation (14) by using the empirical function of C_μ proposed by Ljuboja and Rodi [14] which accounts the damping effect of the wall on the lateral velocity fluctuations (the details of estimating the value of C_μ are given in the Appendix).

Fig. 2(a) compares predicted and measured profiles of $Y_{1/2}$ proposed by Tailland [1] and Guiton [2] at a Reynolds number equal to 18 000. A satisfactory agreement is noted for the three models considered with modified C_μ. In the same way the values of $dY_{1/2}/dX$ obtained with the three low Reynolds number turbulence models with modified C_μ (Table 2) are slightly different, but they all agree with those proposed experimentally by Tailland [1].

In Table 2, we have also compared predicted and measured value of spreading rate $dY_{1/2}/dX$ at a Reynolds number equal to 9600. The agreement with the value of 0.077 [4] is satisfactory for the three low Reynolds turbulence models adopted in this work.

The low Reynolds number turbulence models which allows calculations right to the wall have also the advantage of being able to consider various Reynolds number. This allows us to analyze, according to these numbers, the streamwise evolution of the dynamic jet half width, by adopting the Herrero et al. model [22] with modified C_μ (Fig. 2(b)). The dimensionless parameters suggested by Narashima et al. [7], based on the kinematic momentum flux J discharged by the nozzle and the kinematic viscosity ν of the fluid, were used in this work. The results presented in this figure show that no Reynolds number dependence is noticed on the jet expansion in the similarity region where the flow reaches a local equilibrium which is independent of the detailed conditions at the nozzle. It can be seen from this figure that the present prediction is in good agreement with the reviewed experimental data [4,6].

Table 2
Rate of spread $\frac{dY_{1/2}}{dX}$

References	*Re*	$\frac{dY_{1/2}}{dX}$	
Present investigations		$C_\mu = 0.09$	Modified C_μ
Herrero et al. model [22]	18 000	0.097	0.076
	9 600		0.078
Nagano–Hishida model [23]	18 000	0.093	0.075
	9600		0.076
Chien model [24]	18 000	0.091	0.073
	9 600		0.075
Numerical results			
k–ε model with wall function [14]	–	0.106	0.076
Low Reynolds number stress transport model [21]	10 000	0.071	
Experimental results			
Tailland [1]	18 000	0.076	
Karlsson et al. [4]	9 600	0.077	

Fig. 3 shows the dimensionless profiles of velocity u^+ according to y^+ ($u^+ = u/u_\tau$ and $y^+ = u_\tau y/\nu$), u_τ being the friction velocity expressed according to the wall shear stress τ_w ($u_\tau = \sqrt{\tau_w/\rho}$, with $\tau_w = \mu(\partial u/\partial y)_{y=0}$). These

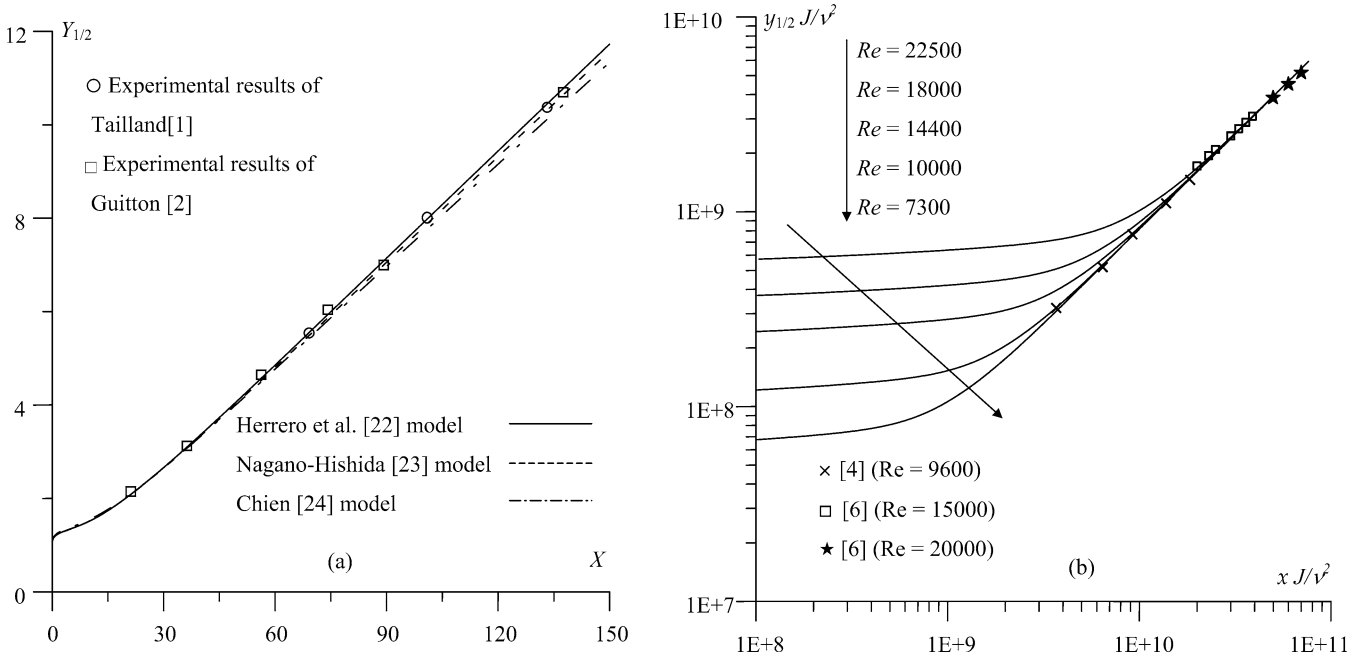

Fig. 2. Streamwise development of the half width: (a) in slot scaling at $Re = 18\,000$; (b) for different Reynolds numbers in momentum scaling.

profiles are presented for the three turbulence models and for a section located in the similarity region of the jet. It is noticed that for low values of y^+ the prediction of u^+ agrees well with the experimental results of Nizou [9]. The wall law $u^+ = y^+$ is thus checked in the near wall region where the molecular viscosity becomes important. For y^+ higher than 10, we note that the various low Reynolds number turbulence models with a standard C_μ ($C_\mu = 0.09$) underestimate the experimental results proposed by Nizou et al. [9]. This figure also shows that the use of modified C_μ, corrects the dimensionless velocity u^+ since the results obtained with the Herrero et al. [22] and Chien [24] models approach to those proposed experimentally by Nizou et al. [9]. On the other hand, with modified C_μ, the Nagano–Hishida model [23] always underestimates experimental results of Nizou et al. [9].

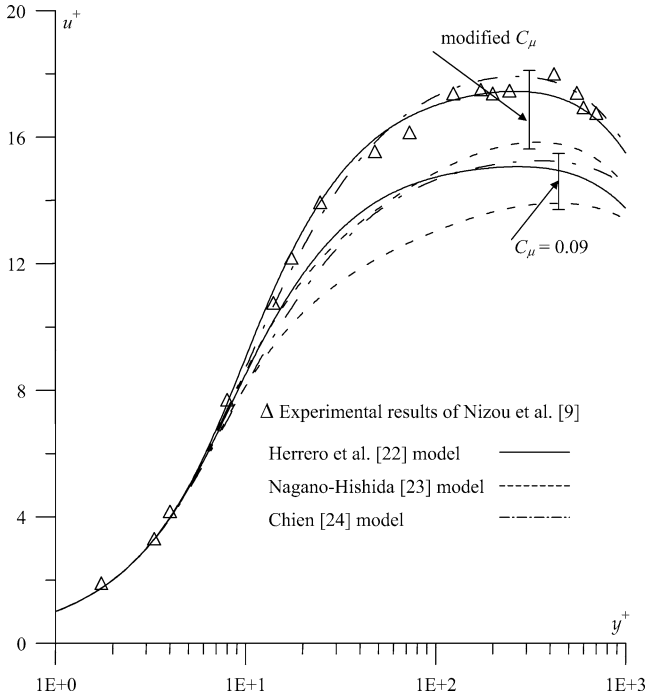

Fig. 3. Dimensionless velocity profiles at $Re = 18\,000$.

The wall friction coefficient C_f, is defined as being the ratio between the wall shear stress and the fluid dynamic pressure: $C_f = \tau_w/(1/2\rho u_m^2)$. In a first stage, we represented in Fig. 4(a), the streamwise evolutions of this coefficient for the three low Reynolds number turbulence models with standard C_μ. It is noted that the latter overestimates C_f compared to the experimental results proposed by Tailland [1]. In a second stage, we represented C_f by using for C_μ the function suggested by Ljuboja and Rodi [14]. The Herrero et al. [22] and Chien [24] models with modified C_μ agree well with the experimental results of Tailland [1], whereas the Nagano–Hishida model [23] always overestimates the wall coefficient friction.

A modified wall friction coefficient defined by $C_f^* = C_f/2(U_m/Re)^2$ is represented in Fig. 4(b) according to $X^* = xJ/\nu^2$, by adopting the Herrero et al. model [22] with modified C_μ. This figure shows that far from the nozzle (similarity region), the evolution of the modified wall friction coefficient is independent of *Re* numbers and depends only on the kinematic momentum flux discharged by the nozzle and the kinematic viscosity of the fluid. In the similarity region our results can be expressed by the following correlation equation: $C_f^* = A(X^*)^N$, with $A = 0.155$ and $N = -1.05$.

The constants A and N suggested above compare quite favorably with the coefficient recommended by Wyganaski et al. [5] ($A = 0.146$ and $N = -1.07$).

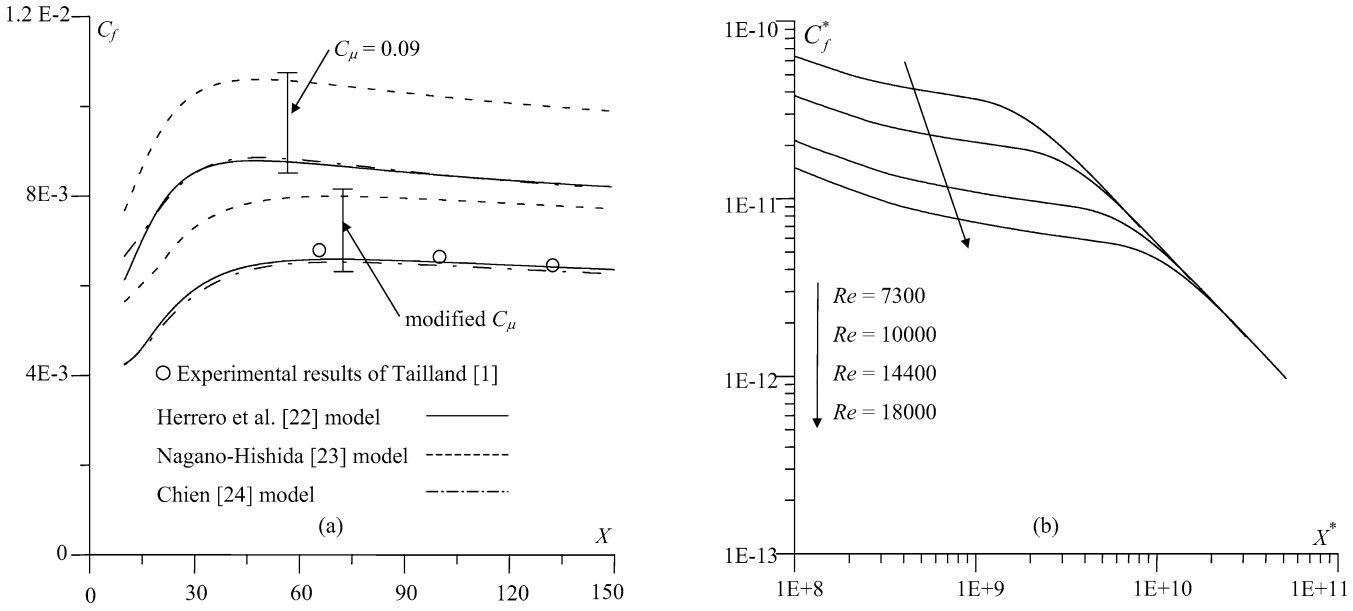

Fig. 4. Streamwise development of the wall friction coefficient: (a) in slot scaling at $Re = 18\,000$; (b) in momentum scaling with different Reynolds numbers.

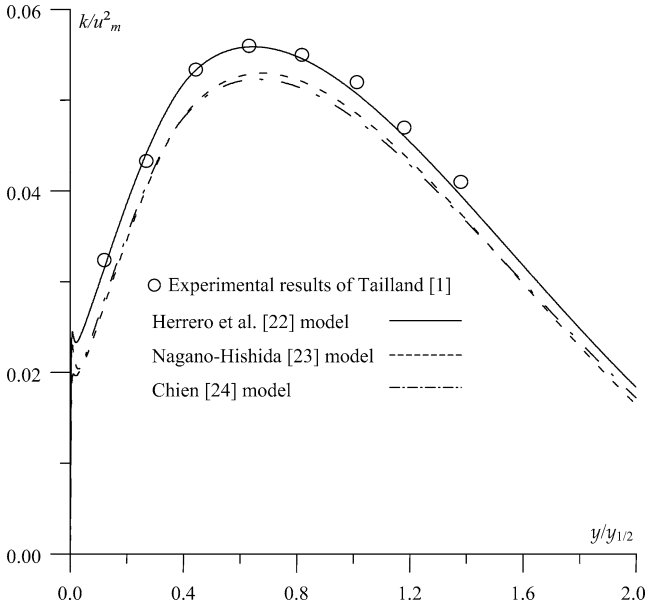

Fig. 5. Transversal evolution of turbulent kinetic energy in the similarity region at $Re = 18\,000$.

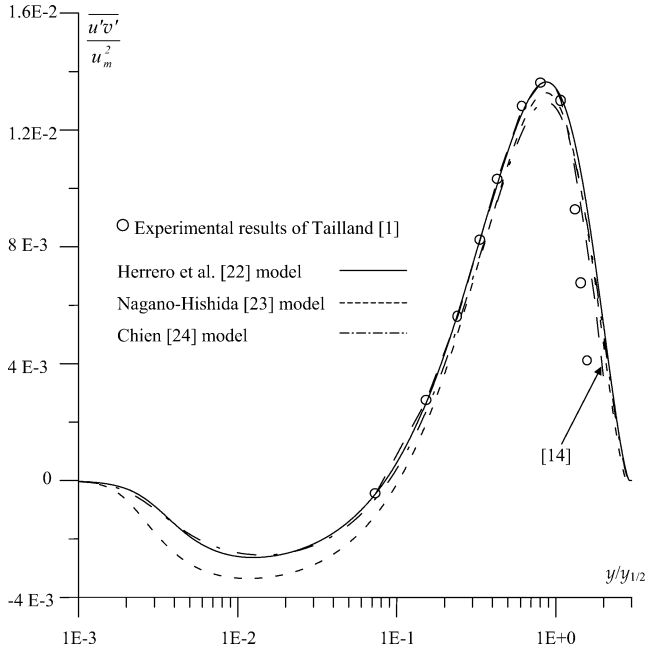

Fig. 6. Transversal evolution of shear stress in the similarity region at $Re = 18\,000$.

3.1.2. Turbulent parameters

Fig. 5 presents the lateral profiles of (k/u_m^2) in the self-similar region of the jet ($X = 85$). This parameter presents a maximum at a distance $y/y_{1/2}$ at the neighborhood of 0.6. A confrontation of our results with those proposed experimentally by Tailland [1], shows that the Herrero et al. model [22] with modified C_μ is more effective to describe the turbulent kinetic energy than the two other models [23, 24].

The lateral distribution of $\overline{u'v'}/u_m^2$ at $X = 85$ is shown in Fig. 6. We notice, for the various low Reynolds number turbulence models, that this parameter is negative in the vicinity of the wall ($y/y_{1/2} < 0.1$): this is due to the positive sign of the velocity gradient in the region located between the wall and the point of maximum velocity. For higher distances of $y/y_{1/2}$, the shear stress increases to reach a maximum located in the jet region. A confrontation of our results with those proposed experimentally by Tailland [1], shows that the Herrero et al. model [22] with modified C_μ is more effective than the two other models to describe the shear stress up to a distance $y/y_{1/2}$ equal to 1.3. For higher distances, our results are slightly higher than the experimental ones [1]. This variation is also observed for the numerical results suggested by Ljuboja and Rodi [14], who used the high Reynolds number turbulence model with modified C_μ.

In this first part, we studied numerically an isothermal wall jet using several low Reynolds number closure turbulence models. A comparison between our results and those proposed experimentally by Tailland [1], Guitton [2], Abrahmsson et al. [6], enables us to conclude that the Herrero et al. model [22] with modified C_μ is the best one to describe the turbulent parameters and the average flow parameters expressed according to the velocity gradient to the wall. The validity of these various closure models will also be analyzed below for the case of a flow evolving in a forced convection regime along a plate submitted to various thermal conditions (uniform heat flux or uniform temperature).

3.2. Non isothermal turbulent wall jet in forced convection regime

In this case, calculations have been made by using a constant turbulent Prandtl number ($Pr_t = 0.85$) [9,27], and for a Prandtl number equal to 0.71. A confrontation of our results with those proposed experimentally by Nizou [8,9] is made to test the validity of low Reynolds number turbulence models in thermal field.

3.2.1. Wall submitted to a uniform heat flux

Fig. 7 shows the lateral profiles of dimensionless temperature T^+ according to y^+. The temperature profiles are given in a section located in the similarity region of the jet by adopting various low Reynolds number turbulence models with modified C_μ for the case of air ($Pr = 0.71$) and for a Reynolds number equal to 14 400. It is noticed that for low values of y^+ ($y^+ < 7$), our numerical results verify well the relation $T^+ = Pr \times y^+$ which is valid in the zone close to the wall. For $y^+ > 7$, a variation is observed between the various evolutions. The transverse profile of T^+ obtained by the Herrero et al. [22] and Chien [24] models with modified C_μ, show a satisfactory agreement with the experimental results suggested by Nizou et al. [8], whereas the Nagano–Hishida model [23] underestimates these results.

For different low Reynolds number turbulence models and for a Reynolds number equal to 14 400, Fig. 8 shows the streamwise development of St/C_f, where $St = h/(\rho c_p u_m)$

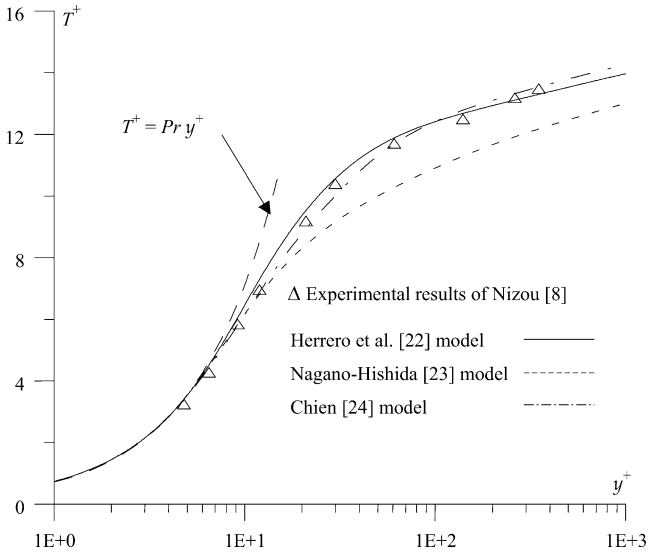

Fig. 7. Dimensionless temperature profiles at $Pr = 0.71$ and $Re = 14\,400$.

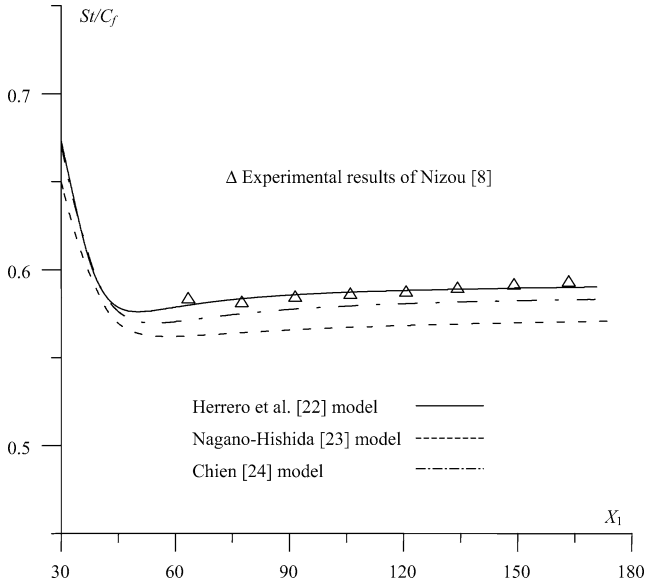

Fig. 8. Streamwise development of St/C_f at $Re = 14\,400$ and $Pr = 0.71$.

is the Stanton number. This figure shows a slight increase in the ratio St/C_f starting from a value of x_1/b equal to 55, which corresponds to a distance x equal to 35 nozzle thickness. This observation, which was also noted experimentally by Mathiew [10] leads to the conclusion that the Colburn analogy is not valid in the case of a turbulent wall jet.

This figure also shows that the Herrero et al. model [22] with modified C_μ describes best the results obtained experimentally by Nizou [8], whereas the two other models of Chien [24] and Nagano–Hishida [23] with modified C_μ, underestimate the ratio St/C_f.

The correlation suggested by Nizou et al. [9] connects the local Nusselt and local Reynolds numbers by the relation $Nu_{x_1} = 0.060 Re_{x_1}^{0.78} Pr^{0.22}$ with $Nu_{x_1} = (hx_1)/\lambda$ and $Re_{x_1} = (u_m x_1)/\nu$. Fig. 9 shows the variation of the local Nusselt number for various Reynolds numbers and for $Pr = 0.71$. It is noticed that in the similarity region, the Reynolds number does not have any influence on the evolution of the local Nusselt number. This figure also enables us to validate our numerical results obtained with the Herrero et al. model [22] by comparing them to the correlation suggested by Nizou [9]. On the other hand, for the Chien model [24], a slight underestimate of Nu_{x_1} compared to the experimental results, is noticed whereas a significant variation is observed compared to the last ones for the results obtained by the Nagano–Hishida model [23].

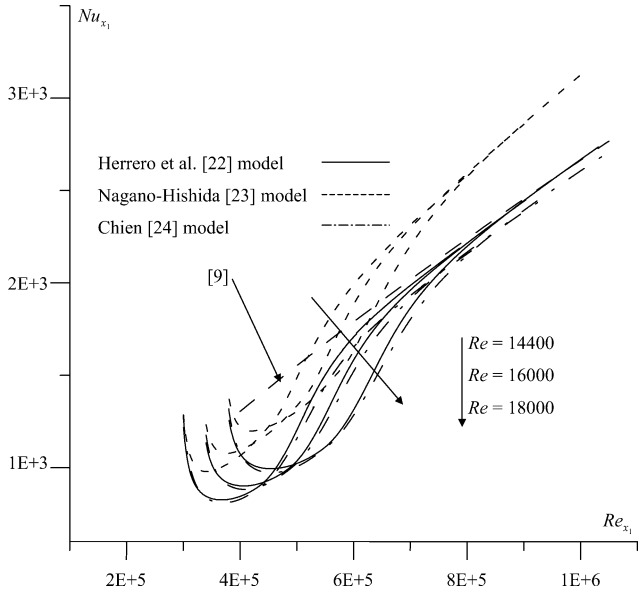

Fig. 9. Streamwise development of local Nusselt number with local Reynolds numbers at $Pr = 0.71$.

3.2.2. Wall submitted to a uniform temperature

The streamwise evolutions of the analogy Reynolds factor (St/C_f), and the local Nusselt number, are given and compared with those obtained by imposing a uniform heat flux boundary condition on the wall. The turbulence model of Herrero et al. [22] with modified C_μ [14] is adopted.

In Fig. 10, we have presented the streamwise development of (St/C_f) for a Reynolds number equal to 14 400. It is noticed that this parameter is always lower than the value obtained for a uniform heat flux. This observation was experimentally validated by Reynolds [28] who has proposed for St/C_f a value of about 0.577. This is in agreement with our results since this parameter is close to 0.575.

The streamwise development of the local Nusselt number according to the local Reynolds number (Re_{x_1}), for the two boundary wall conditions, is given on Fig. 11 for a Reynolds number equal to 14 400. The observations announced for the variation of the Nusselt number for a uniform heat flux are also valid for a uniform temperature. The evolution of local Nusselt number according to the local Reynolds number verifies the following relation: $Nu_{x_1} = 0.056 Re_{x_1}^{0.78} Pr^{0.22}$.

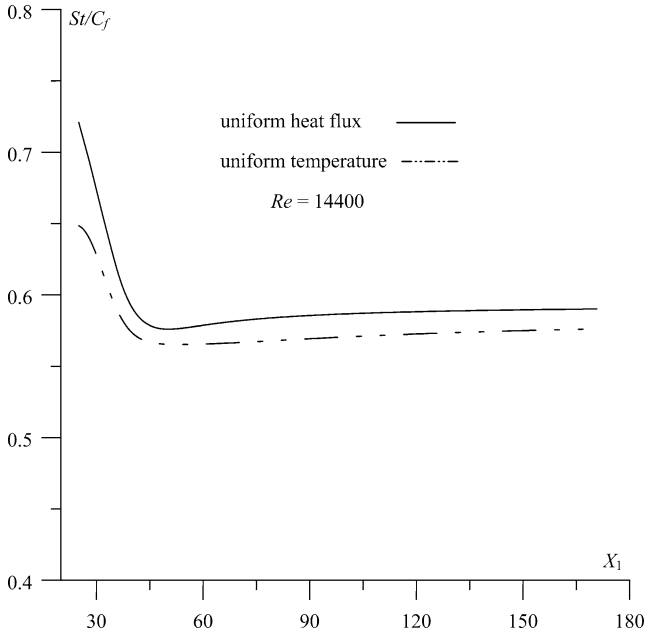

Fig. 10. Streamwise development of St/C_f for two boundary conditions on the wall.

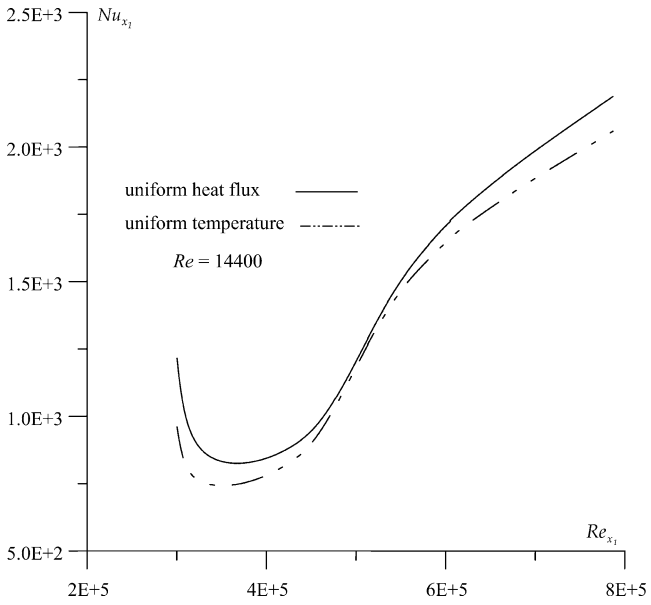

Fig. 11. Streamwise development of local Nusselt number for two boundary conditions on the wall.

It is also noted that the thermal boundary condition on the wall influences the evolution of the Nusselt number in the different regions of the wall jet. The heat transfer in the case of an isothermal wall jet is always lower than that observed in the case of a wall submitted to a uniform heat flux.

4. Conclusion

In this work, we have studied numerically a turbulent plane two-dimensional wall jets in quiescent surrounding. A finite difference method with a non-uniform grid was carried out to solve the problem by using the boundary layer assumptions and various low Reynolds number closure models were used.

The discussion carries essentially on the validity of low Reynolds number turbulence models [22–24] to describe the dynamic, thermal and turbulent parameters of this type of flow.

For the case of an isothermal wall jet, the comparison of the half width obtained with the three low Reynolds number turbulence models [22–24] with those proposed experimentally by Tailland [1] and Guitton [2] have showed that these models overestimate this parameter by about 20%. The solution adopted to solve this problem consists in replacing the constant C_μ, appearing in the Kolmogorov–Prandtl relation by the formulation suggested by Ljuboja and Rodi [14]. This approach allowed the different tested models to better predict the expansion of the wall jet since a satisfactory agreement is observed with the results suggested experimentally by Tailland [1] and Guiton [2].

The low Reynolds number turbulence model [22] allows us to validate the experimental observations of Wygananski et al. [5] and Abrahmsson et al. [6] who suggested that, in the similarity region, the dynamic wall jet half width as well as the wall friction coefficient depend only on the momentum flux discharged by the nozzle exit and the kinematic viscosity of the fluid.

For a non-isothermal turbulent wall jet, we have compared our results with those proposed experimentally by Nizou et al. [8,9], in forced convection regime for the case where the wall is heated by a uniform heat flux. It is shown once again that the modified Herrero et al. model [22] is more effective to determine the thermal characteristics of the flow. We were able also to put into evidence, for two different thermal conditions at the wall (uniform temperature or uniform heat flux), a slight increase in the analogy Reynolds factor (St/C_f), which leads us to conclude that the analogy of Colburn is not valid in the case of a turbulent wall jet.

Appendix

The C_μ function proposed by M. Ljuboja and Rodi [14] is computed from the following expression:

$$C_\mu = 0.09 G_1 G_2$$

with

$$G_1 = \frac{1 + \frac{3}{2}\frac{c_2 c_2'}{1-c_2} f}{1 + \frac{3}{2}\frac{c_1'}{c_1} f}$$

and

$$G_2 = \frac{1 - 2\frac{c_2 c_2' \frac{P}{\varepsilon}}{c_1 - 1 + c_2 \frac{P}{\varepsilon}} f}{1 + 2\frac{c_1'}{c_1 + \frac{P}{\varepsilon} - 1} f}$$

The function f is estimated by the following formulation: $f = \frac{k^{3/2}}{c_w y\tilde{\varepsilon}}$ whereas the turbulent kinetic energy production P is given by the expression below:

$$P = -\overline{u'v'}\frac{\partial u}{\partial y}$$

The constants used for the C_μ formulation are:

$$c_1 = 1.8; \quad c_2 = 0.6; \quad c_1' = 0.6; \quad c_2' = 0.3; \quad c_w = 3.72$$

References

[1] A. Tailland, Contribution à l'étude d'un jet plan dirigé tangentiellement à une paroi plane, Doctoral Thesis, Université de Lyon, 1970.

[2] D.E. Guitton, Some contributions to the study of equilibrium and non-equilibrium wall jets over curved surfaces, Ph.D. Thesis, McGill University, 1970.

[3] R.I. Karlsson, J. Eriksson, J. Persson, LDV measurements in a plane wall jet in a large enclosure, in: 6th International Symposium on Applications of Laser Techniques to Fluid Mechanics, Lisbon, 1992, pp. 151–156.

[4] 6th ERCOFTAC/IAHR/COST Workshop on Refined Flow Modelling: Case 5.1. The 2D plane turbulent wall jet organised by Professors Hanjalic and Obi, 1997.

[5] I. Wygananski, Y. Katz, E. Horev, On the applicability of various scaling laws to the turbulent wall jet, J. Fluid Mech. 234 (1992) 669–690.

[6] H. Abrahmsson, B. Johannsson, L. Lofahl, A turbulent plane two-dimensional wall jet in a quiescent surrounding, European J. Mech. B Fluids 13 (1994) 533–556.

[7] R. Narasimha, K.Y. Narayan, S.P. Parthasarathy, Parametric analysis of turbulent wall jet in still air, Aero. J. 77 (1973) 355–359.

[8] P.Y. Nizou, Analogie entre transferts de chaleur et de quantité de mouvement dans un jet pariétal plan turbulent, Internat. J. Heat Mass Transfer 27 (1984) 1737–1748.

[9] P.Y. Nizou, Tida, Transferts de chaleur et de quantité de mouvement dans les jets pariétaux plans turbulents, Internat. J. Heat Mass Transfer 38 (1995) 1187–1200.

[10] J. Mathieu, Contribution à l'étude aérodynamique d'un jet plan évoluant en présence d'une paroi, Publications scientifiques et techniques du Ministère de l'air, No 374, 1962.

[11] W.S. Yu, H.T. Lin, H.C. Shih, Rigorous numerical solutions and correlations for two dimensional laminar buoyant jet, Internat. J. Heat Mass Transfer 35 (1992) 3389–3395.

[12] H. Mhiri, S. El Golli, G. Le Palec, Ph. Bournot, Influence des conditions d'émission sur un écoulement de type jet plan laminaire isotherme ou chauffé, Rev. Gén. Therm. 37 (1998) 898–910.

[13] B.E. Launder, D.B. Spalding, The numerical computation of turbulent flow, Comput. Methods Appl. Mech. Engrg. 3 (1974) 269–289.

[14] M. Ljuboja, W. Rodi, Calculation of turbulent wall jets with an algebraic Reynolds stress model, J. Fluids Engrg. 102 (1980) 350–356.

[15] B.E. Launder, G.J. Reece, W. Rodi, Progress in the development of a Reynolds stress turbulence closure, J. Fluid Mech. 68 (1975) 537–566.

[16] K. Hanjalic, B.E. Launder, A Reynolds stress model of turbulent and its application to thin shear flows, J. Fluid Mech. 52 (1972) 609–638.

[17] 6th ERCOFTAC/IAHR/COST Workshop on Refined Flow Modelling: Case 6.1. The three dimensional wall jet organised by Professors Hanjalic and Obi, 1997, pp. 75–85.

[18] W. Kebede, M.Sc. Thesis, UMIST, Dept. Mech. Eng., 1982.

[19] T.J. Craft, B.E. Launder, On the spreading mechanism of the three-dimensional turbulent wall jet, J. Fluid Mech. 435 (2001) 305–326.

[20] H. Abrahamsson, B. Johansson, L. Lofdahl, An investigation of the turbulence field in the fully developed three-dimensional wall-jet, Internal Rep. 97/1, Chalmers University of Technology, Sweden.

[21] T.J. Craft, Computation of plane and 3-dimensional wall jets, in: The 8th Biennal UMST CFD Colloquium, Turbulence Modelling Applied, 1998.

[22] J. Herrero, F.X. Grau, J. Grifoll, F. Giralt, A near wall k–ε formulation for high Prandtl number heat transfer, Internat. J. Heat Mass Transfer 34 (1991) 711–721.

[23] Y. Nagano, M. Hishida, Improved form of the k–ε model for wall turbulent shear flows, J. Fluids Engrg. 109 (1987) 156–160.

[24] K.Y. Chien, Predictions of channel and boundary layer flows with a low-Reynolds number turbulent model, AIAA J. 20 (1982) 33–38.

[25] H. Mhiri, H. Sabra, S. El Golli, G. Le Palec, P. Bournot, Etude numérique des conditions d'émission sur un écoulement de type jet plan turbulent isotherme ou chauffé, Internat. J. Therm. Sci. 38 (1999) 904–915.

[26] H. Sabra, H. Mhiri, S. El Golli, G. Le Palec, Ph. Bournot, Etude numérique des conditions d'émission sur un écoulement de type jet axisymétrique turbulent, Internat. J. Therm. Sci. 40 (2001) 497–511.

[27] B.A. Kader, A.M. Yaglom, Heat and mass transfer laws for fully turbulent wall flows, Internat. J. Heat Mass Transfer 15 (1972) 2329–2351.

[28] W.C. Reynolds, W.M. Kays, S.J. Kline, Heat transfer in the turbulent boundary layer, NASA Memorandum, 12-1-58W, 12-2-58W, 1958.